

INVESTIGATION OF THE APPLICATION OF AUSTENITIC FILLER METALS IN PAVED TRACKS FOR THE REPAIR OF THE RUNNING SURFACE DEFECTS OF RAILS CONSIDERING FIELD TESTS

András Brautigam^{1,2}, Szabolcs Szalai³, Szabolcs Fischer¹

¹Széchenyi István University,
Department of Transport Infrastructure and Water Resources Engineering, Hungary
²Budapest Transport Privately Held Corporation (BKV), Hungary
³Széchenyi István University,
Department of Vehicle Manufacturing and Technology, Hungary

Abstract. *The current study aims to define a welding technology that allows for the repair of normal and heat-treated rails in paved tracks with partial dismantling and partial preheating in such a way that the resulting layer is not susceptible to cracking and can be done with minimal dismantling, even during night shifts or while traffic is present. High-elongation austenitic consumables (capable of approximately 2-3 times greater elongation than rails; rails have approximately 8-14% elongation) were used and tested for this purpose. Welds and rail tread defects were repaired on Hungary's busiest tram line (12-14 million gross tons per year), which also has a high axle load compared to other European tram lines. The repairs were performed on various rail grades using different layer numbers, and the experimental consumables were compared to conventional hardfacing welding methods. Welds were continuously monitored after welding, and surface hardness measurements were taken. A hardening function and an applicable technology were defined based on the results. The function compares the through-rolled axle tons to the expected hardness values over the first 6 million tons. Partial preheating and partial track disassembly can be used to weld a layer of hardness equal to the hardness of the rails and wheels.*

Key words: *Rail, Build-up welding, Austenitic, Hardfacing, Hardness, Running surface, Paved track, Tramway*

Received: August 28, 2023 / Accepted October 03, 2023

Corresponding author: Szabolcs Fischer

Department of Transport Infrastructure and Water Resources Engineering, Faculty of Architecture, Civil Engineering and Transport Sciences, Széchenyi István University, H-9026 Győr, Egyetem tér 1., Hungary
E-mail: fischersz@sze.hu

1. INTRODUCTION

Long-distance train travel became a popular mode of land transportation in the twentieth and twenty-first centuries [1-3]. It is convenient, safe [4], quick, and usually on time; however, this depends on the country and train operator. Long-distance train travel is less competitive than air travel beyond 500-1000 km in terms of journey time [5]. Travel costs, particularly ticket and season ticket rates, put it at a competitive disadvantage compared to low-cost airlines. Railway development in the eighteenth and nineteenth centuries, on the other hand, enabled great cities to build railway and passenger terminals in the inner core, even in old city centers. Airports are frequently located outside of cities. It could be anywhere between 10 and 50 kilometers long. Tourists and tourism suffer because these long distances necessitate more public or private transportation. Risk assessments are required for potential projects. Given the impact of risk events on infrastructure project costs, timeliness, and quality, investment in risk management is required to avoid or mitigate negative consequences [6].

Rising energy and fuel prices (diesel, kerosene, etc.) will pose significant challenges to countries and public and private (large) public transportation businesses in 2021-2023. In fact, there are additional reasons for this. Among the causes and explanations are the global political crisis, the COVID-19 epidemic, and the cyclical stock market boom and crash. Because no single factor can be overlooked, the most likely answer is a combination of the above.

Transportation, particularly rail transit and railway lines [7,8], is critical to the national economy.

It is worth noting that electric road vehicles have grown in popularity in recent years, primarily for private transportation [9,10] (another "fancy" direction is the group of autonomous vehicles [11]). Electric buses can provide urban-suburban bus services in the short term in the case of public transportation [12]. (When considering electric vehicles, battery analysis is also an important research area [13,14].) BENIP (Built Environment Information Platform) is a remarkable initiative in infrastructure planning, development, and research [15]. BENIP depicts the theoretical and practical aspects of the interconnected and chained world of engineering in the built environment, ranging from the smaller entities of architecture (buildings) to the civil engineering domain (complex structures) to the vast transportation systems.

The current paper is about the use of austenitic filler metals in paved railway tracks to repair running surface defects. The authors then compiled relevant findings from the international literature on this specific research field.

Consumables and base metals with austenitic microstructures are widely used in a variety of industries, from mining to automotive and defense, due to advantageous properties such as high elongation (> 35%), high resistance to cracking compared to rails, and surface hardening ability. Austenitic plates have long been known in the mining industry for their advantageous properties and are preferred for their hardening properties, as they can harden from an initial hardness of 200 HV (HV unit means Vickers hardness that equals 199 Brinell hardness [HB]) up to 580 HV (513 HB) [16]. The military industry also uses consumables for armor plates (MiiLux Protection 500 material). Gürol's research [17] focuses on fillet welding methods on high-strength MiiLux Protection 500 steel, used as an armor material in the defense industry. Elements mapping methodologies, microstructural analysis, and microhardness testing were used to describe the welded

constructions. The study discovered that using ferritic and austenitic filler metals with GMAW (gas metal-arc welding) at low heat input successfully coupled the weld metal and HAZ (heat-affected zone) [17].

Several foreign studies have already looked into the hardness values of rails and rail welds, as well as the interactions between wheels and rails.

Molyneux-Berry et al. [18] discuss the impact of wheel/rail contact conditions on the microstructure and hardness of railway wheels. The observed hardness and microstructure variations, as well as the stress history at the wheel/rail contact (derived from dynamic simulations), are discussed. The wheel/rail interactions generate stresses that exceed the material yield stress between 1 and 7 mm depth, resulting in work hardening without a macroscopic change in microstructure. The underlying hardness trend is linked to wheel manufacturing procedures as well as microstructural variations like proeutectoid ferrite content and pearlite lamellae spacing.

Liu et al. [19] provide another example of wheel-rail interaction. An experiment on the wear and damage behaviors of machined wheel/rail materials under dry rolling-sliding conditions is carried out using twin-disc wear testing equipment. Rail discs have slightly higher surface hardness after machining than wheel discs, but turned wheel discs have significantly higher surface roughness and plastic deformation layer. Wheel discs wear out significantly faster than rail discs.

The surface damage morphology of wheel discs differs significantly from that of rail discs, with adhesive wear, spalling, peeling, and fatigue cracks dominating. Wheel discs wear out faster than rail discs, but rail material is more wear-resistant. The surface hardness, surface roughness, and plastic deformation layer of wheel/rail discs all have an impact on wear behavior after machining, with friction pairings with the appropriate original surface hardness and roughness providing the most minor wear loss. When the tested #W2 specimens (samples) make rolling-sliding contact with the rail discs, abrasion resistance improves overall.

Bozkurt [20] investigated the tribological characteristics of the R260 rail quality for the rail head, web, and foot. He discovered that the third material (water, humidity, lubricant, debris, or a combination of these elements) between them has a significant influence on the wheel-rail contact, resulting in a rail coefficient of friction between 0.35 and 0.39. It was also demonstrated that the hardness values decrease continuously as a function of distance from the rail head to the rail foot, with an average hardness of 353 HB on the rail head, 316 HB on the rail web, and 278 HB on the rail foot after the tests. Apart from the pearlitic microstructure typical of R260 rails, microstructural investigations revealed that the rail foot contains the most ferrite.

Protsenko et al. [21] proposed determining the optimum rail grinding parameters after investigating the tribological properties. Rail grinding is a preventative maintenance procedure that removes problematic material layers from the rail surface while preserving the size, shape, and surface quality. This work aims to determine the effect of grinding on the rail surface's tribological properties and establish the optimal grinding process parameters to ensure the best rail surface wear resistance. The best process parameters for increasing rail surface wear resistance are 0.007 mm depth of cut, 30 m/s grinding wheel speed, and 20 °C rail temperature (it is best to treat rails during the warm season).

Additional tribological research revealed that sliding wear of rail and wheel steels is simulated using a pin-on-disc test model system that simulates contact wear between the wheel flange and the rail gauge corner. Normal load variation was used in both dry and

lubricated trials. The researchers discovered that while pair hardness had no effect on the mass loss of the tribosystem studied under dry conditions, mass loss was significantly lower in lubricated testing than in other tests. This emphasizes the technological significance of implementing wheel flange lubrication, improving rail lubrication operations, and revising wheel standards and/or specifications [22].

Cracks appeared in the heat-treated rails during pre-bending before installation during the construction of the Zagreb tramway line, which were later tested [23]. Despite significant variations in the rail cross-section, the hardness values were higher than the minimum values required (on average, 24% higher). It was also discovered that the heat-treated rails' hardness or tensile strength values did not cause the defects.

Poznyakov et al. [24] investigated crack initiation prevention. The study focuses on the properties of rail steel welded joints in electric arc welding, specifically the effect of the thermo-deformational cycle of welding (TDCW) on structural changes, strength, and ductility qualities of HAZ metal in rail steel welded joints containing 0.72% carbon. This hardened metal is strong but ductile, making it challenging to prevent cold cracks from forming in joints without preheating to 250 °C.

Konstantinova et al. [25] investigated the possibility of hardening the side surface of the rail head with plasma surface quenching to avoid frequent rail replacement due to wear during heavy traffic. The surface 2.5-3 mm thick layer was successfully hardened to 450-830 HV (419-600 HB) in the experiments, but martensite was already present in the microstructure. The results are expected to increase in-service life by 2-3 times.

Woodhead [26] concentrated on determining how different material properties affect rolling contact fatigue (RCF) and rail steel wear. Hardness is a good predictor of tensile strength, and steel samples from the head and foot of rails have significantly different yield strengths (24%). The examinations showed that the ratio of the product of Young's modulus squared and percentage elongation to hardness cubed ($E^2 \times Pe / H^3$) had a much better correlation ($R^2=0.98$) to wear data than just hardness ($R^2=0.89$), where E is the Young's modulus [Pa], Pe is percentage elongation [%], and H is the hardness [HB].

The above study confirms that there has been a lot of research on rail hardnesses and their interactions with railway wheels, but no studies have shown the application of austenitic filler materials on the rails' running surfaces.

With ever-increasing urban traffic, track maintenance is becoming increasingly difficult. Developing technology for repairing running surface defects has become necessary for paved tracks, which can be accomplished through partial preheating and partial track dismantling (removing the embedding pouring to the bottom of the rail head). The complete dismantling, welding, and "re-pouring" of the embedding pouring in a paved track, as well as the embedding pouring's binding time, can take anywhere from 24 hours to a whole weekend. In contrast to the requirements outlined above, welding can be performed even during nighttime shutdowns (and, in some cases, during traffic) because the short period of partial dismantling does not cause structural and geometric stability issues in the track. As rail quality improves, the carbon content of the base material rises (and vice versa), necessitating the highest possible preheating temperature (350-400 °C) to avoid rapid cooling and cracking. Given that the embedding pourings in paved tracks already melt at 100-120 °C, a consumable that does not require such a high preheating temperature and does not cause cracking in the weld and base material was required. Traditional hardfacing materials used for rail build-up welding do not meet these

requirements but are met by austenitic 18-8-6 materials (18% Cr, 8% Ni, 6% Mn, or higher alloying content).

The authors set out to thoroughly investigate the technology described above in a real railway track environment with traffic loads. For this purpose, repair welds were prepared on a tramway track in Budapest (Hungary), where the annual traffic load on the line is relatively high. The welds were carried out in accordance with the most stringent technological standards. Welding repairs for the austenitic build-up and control hardfacing were also carried out. Approximately 5.5 million gross tons were rolled through the sections during the five-month test period. Hardness measurements were taken 85-120 cm from the welds' center axis at a resolution of 5 cm. The degradation-change functions were computed as a function of the axle tons. The findings may be helpful in railway track maintenance, where a new type of austenitic build-up repair welding may be considered an alternative to traditional repair technologies.

The paper is structured in the following way. Section 2 discusses the problem statement and additional literature review that are closely or tangentially related to this topic, as well as their relevant findings and results for the current article. Section 3 summarizes the materials and methods used in the study. Sections 4 and 5 deal with the findings and discussion, respectively. Section 6 discusses the main conclusions drawn from the experiments and investigation.

2. PROBLEM STATEMENT AND FURTHER LITERATURE REVIEW

The authors have chosen to supplement the brief literature review presented in Section 1 with a more detailed analysis in this section to obtain a more complete picture of the relevant research results in the research area.

Austenitic filler materials have been used for decades in three areas of the railway industry, one of which is the repair of Hadfield steels by build-up welding (see Table 1 and Fig. 1). The second major group is the welding of R220 grooved rails in the factory and on the track to reduce side wear and noise emission [27]. The welding factory mills the most worn parts of the rail head (the area bounded by the running surface and the running edge, the area where the wheel contacts the rail head, and the area where the check rail contacts the wheel sidewall) to prepare the nest into which the austenitic filler material is welded (see Table 2 and Fig. 2). This layer not only helps to reduce noise, but it is also more resistant to abrasion wear than the base rail grade when hardened by vehicle traffic. Figure 3 depicts the layer applied at the rail in the track. Furthermore, these filling materials in Group 3 act as a buffer layer beneath the hardfacing layer. Build-up weldings are used to prepare them for railway crossings and other rail defects.

Table 1 Chemical composition of the austenitic manganese steel electrode

Chemical composition [%]									
	C	Si	Mn	P	S	Cr	Ni	V	Nb
min.	0.60	0.50	11.10	-	-	-	-	-	-
max.	1.20	1.10	14.90	0.05	0.01	0.10	0.10	0.10	0.10



Fig. 1 Repair of a turnout frog from Hadfield steel. A – defect, B – preparation, C – welded structure

Table 2 Chemical composition of austenitic solid wire

Chemical composition [%]				
C	Si	Mn	Cr	Ni
0.08	0.9	7.0	19.2	9.0



Fig. 2 Build-up welding on grooved rails to reduce wear

The European standards for Vignol [28] and grooved [29] rails specify a minimum hardness value for the rail head to indicate steel grade (for example, R260 has a minimum hardness of 260 HB) but allow for a range within the rail head hardness to be met before installation.



Fig. 3 Austenitic layer in the rail surface

Table 3 Steel grades and their surface hardness values according to EN 13674 (Vignol rails) [28]

Steel grade	The hardness of the rail running surface center line [HB]
R200	200 to 240
R220	220 to 260
R260	260 to 300
R260 Mn	260 to 300
R320 Cr	320 to 360
R350 HT	350 to 390
R350 LHT	350 to 390
R370 CrHT	370 to 410
R400 HT	400 to 440

Table 4 Steel grades and their surface hardness values according to EN 14811 (grooved rails) [29]

Steel grade	The hardness of the rail running surface center line [HB]
R200	200 to 240
R220 G1	220 to 260
R260	260 to 300
R290 GHT	290 to 330
R340 GHT	340 to 390

International articles closely or tangentially related to this topic, as well as their relevant findings and results for the current article, are detailed in the following paragraphs.

Kou [30] thoroughly reviewed the literature on detecting and evaluating rail surface defects. Surface rail defects can cause wheel wear, increased derailment risk, and safety concerns. Early detection is critical for railway safety and service life extension. Several approaches to defect inspection have recently been investigated, including ultrasonic and acceleration detection, computer vision, and deep learning. Machine learning visual inspection techniques are commonly used to detect railway surface problems. Using multiple methodologies to detect discrete defects improves detection. For difficult tasks, more research is needed to detect rail surface crackings with an accuracy of 75% to 85%.

Long-term rail surface deterioration research on the Swedish iron-ore line was conducted, considering maintenance interventions [31]. The FR8RAIL running gear was

found to be superior overall, with cross-bracing and a softer primary suspension being especially noticeable for curve radii greater than 600 m. The possibility of extending the grinding interval and reducing track damage is highlighted.

Another study investigates using Consumable Guide Enclosed Arc Welding (CGEAW) technology to arc weld rail profiles [32]. CGEAW uses a specially designed electrode and self-shielded flux-cored wire, making it portable, easy to manufacture, and capable of high filler material deposition rates. The required gap between welded rails is 12-16 mm, which can be used to calculate process efficiency.

The research [33] looks into the structural phase transition of rail steel in compression, examining its structure and inadequate substructure to 50% uniaxial compression. Cold hardening is discovered to be a multi-stage process, with pearlite grain fragmentation increasing with deformation. Carbon atoms are transported out of the cementite crystal lattice and form tertiary cementite particles with sizes ranging from 2 to 4 nm. Due to dislocation delay by cementite particles, a non-uniform dislocation substructure emerges during steel deformation.

In 2019, the authors of [34] investigated the genesis and progression of contact-fatigue cracks in rail wear. After designing and manufacturing an experimental setup, a two-hour fault detection test program was carried out using fluorescent magnetic particle inspection. Contact-fatigue cracks form in the rail head after approximately 200 thousand load cycles, consistent with other studies showing similar damage after 190-290 thousand cycles. The primary cause of rail head contact-fatigue faults is insufficient rail steel contact-fatigue strength.

The research [35] also investigates the mechanical properties and fatigue characteristics of two types of wheels and rails, emphasizing how they affect wear and contact fatigue. The KS60-rail and UIC60-rail had higher yield strength and hardness with lower elongation than the RSW-wheel and R7-wheel. The crack toughness of the KS60-rail was 73 MPa m^{-2} , 1.8 times greater than the UIC60-rail's 41 MPa m^{-2} crack toughness. The UIC60-rail and R7-wheel outperformed the KS60-rail and RSW-wheel regarding wear resistance.

The study [36] investigates the dynamics of welded rail gap and rail base hardness using a semi-infinite rod and elastic-based damping. It finds both static and dynamic solutions, indicating that the dynamic factor does not exceed 1.5 during rail breakdowns. On an elastic basis, the paper also generates equations for the thermal deformation of a jointless track with a stiffness-varying insert. Although a rigid insert of up to 20% of the rail's length has no effect on the track's stress-strain state (SSS), it may increase clearance for unintended rail breaks, reducing traffic safety. According to the study, a 10-12 cm gap is possible at random kink rail.

Gertsyk and Volgina's [37] article investigates the causes and types of rail track degradation, as well as rail manufacturing processes such as heat treatment, end treatment, surface hardening, and anti-flake treatment. Several procedures, including volumetric quenching with oil cooling and subsequent tempering, thermal rail hardening with tp. heating (high-frequency current), complicated deoxidizers, high carbon content steels, and continuously cast billets have been proposed to improve rail track endurance. These techniques are intended to reduce flock sensitivity while increasing rail track hardness.

Fischer et al. [38] investigated the heat-affected zone of various thermit rail weldings. They considered the rail grades R260 and R400HT. Their first sample was R260-R400HT with a normal non-heat-treated welding portion for R260 rails, and their second sample

was R260-R400HT with a heat-treated welding portion for R350HT rails. The critical technological directions were strictly adhered to. Based on the results of the laboratory hardness, macro-, and microstructural tests, Sample #2 performed better in running the hardness profiles. It indicates that if temporary intermediate hardness rails cannot be incorporated, welding in the two-step rail grade leap with the welding section corresponding to the intermediate rail is preferable. To summarize, more laboratory testing will be needed in the future, where it would be worthwhile to investigate several cases between R200 and R400HT (considering special, for example, bainitic rails, etc.), not only for Vignole rails but also for grooved rails and block rails.

Jovanovc et al. [39] investigated the use of an excavator on railway tracks. They examined this mechanical structure using materials science, metallurgy, and mechanical engineering, which frequently overlap in this paper. Steels, which are iron alloys containing carbon and other elements, are indispensable in these disciplines due to their versatility and wide range of properties. In materials science, they are studied microstructurally to discover the relationships between their composition, processing methods, and properties. Metallurgy is the refinement of the extraction and alloying processes to produce steels with specific properties suitable for various applications. Mechanical engineers frequently use these well-characterized steels in their designs and projects where strength, durability, and cost-effectiveness are critical factors. Welding is a common technique for joining steel parts in these fields. Welding is a material-coalescing process required for assembling and repairing many steel structures and components, making it an essential aspect of these fields of study and practice.

Tica et al. [40] used the sophisticated design software DVOBRZ to discuss reversible planetary gearsets controlled by two brakes for internal combustion railway vehicle transmission applications. This software can be used to design welding machine components and/or welding processes. A carefully planned design process must be fulfilled before determining the required material (steel and metal) qualities. They are critical in the adequate and appropriate mechanical engineering preparatory process. Considering a gearset's wear and resistance to wear, as well as the associated design steps, necessitates similar engineering thinking as analyzing the relationship between a railway wheel and a rail. It can only be considered tangentially for this article up to the point where the base steel material is considered. Welding is very rarely used to repair gearset components. However, it is possible to apply a wear-resistant coating to extremely resistant to wear components and elements, and it is also possible that they and their microstructural changes associated with hardness increase may occur during use.

Monek and Fischer [41] investigated the use of digital twins in smart manufacturing. This paper presented a digital twin model of a research and demonstration platform in a DES (discrete event simulation) environment that improved the connection between the physical and digital layers through data acquired by a smart workpiece with an embedded IMU (inertial measurement unit) sensor. Without user intervention, the system may detect anomalies such as a jammed workpiece or a reduced conveyor speed. The authors created an easy-to-use framework with a user interface for visualization, process monitoring, and troubleshooting. The goal is to create a modular framework that can be used by both small and medium-sized businesses and large corporations. Merging smart product and PLC data with machine learning support enables high-precision workpiece state identification and motion prediction, with 98.7% accuracy on training data and 98.45% on test datasets. The extended digital twin framework for typical DES simulations can improve synchronization

between the digital twin and the physical system, detect anomalies, and reduce input data collection time. The importance of the cited article stems from the fact that the repair welding presented in this article can be automated and created in a computer environment, serving as its digital twin. However, because the use of IMU in welding can be problematic (high temperatures, vulnerable or fragile parts, placement to avoid getting in the way of any technological process, etc.), further development of the solution is definitely warranted.

Ovchinnikov et al. [42] investigated the possibility of extending rail service life in case of a rail head defect. They discussed how rails are subjected to wear, corrosion, and contact fatigue, all of which cause flaws and damage. The size, location, and direction of flaws determine the residual life of rails. This article uses the finite element method to estimate the maximum permitted crack-size values and investigates crack plane orientation. It is discovered that the stress intensity factor is location-dependent, allowing safe operation on low-activity railroads. The FEM simulation model considers internal strains caused by different crack sizes and orientations. Pultznerová et al. [43] investigated the effect of railway superstructure conditions on traffic noise on the regional line. In their research, they only looked at Slovak railway lines. There is now an effort to upgrade not only major railway lines but also minor ones. This is also true for the Poltár-Uteká line segment, where the sleepers are in poor technical condition and will be replaced with a Y-type sleeper soon. The new construction's impact on the sleeper's noise output should also be assessed. It can be stated that the running surface of the rails, rather than the condition of the sleepers, has the most significant impact on noise emission. Taking these factors into account may necessitate additional research.

The impact of traction electricity (TE) consumption factors on driving speeds and energy consumption in rail transportation is investigated by Kampczyk et al. [44]. It employs expert techniques and a novel TE consumption calculation to analyze the movement resistances of electric locomotives during braking and starting. The findings show a significant relationship with the speeds of existing catenary-supplied electric vehicles. This innovative technique advances engineering and technical disciplines, particularly civil engineering, surveying/geodesy, and transportation. Better quality rail repair weldings, of course, improve the geometric condition of the railway track and slow geometric degradation at these critical locations. The task of infrastructure managers is to ensure that the infrastructure they manage and operate is in the best possible condition at the lowest possible cost. The lower the additional traction energy, the better the condition of the railway track. Of course, other influencing factors and aspects should not be overlooked [45].

3. MATERIALS AND METHODS

The chosen site is not only the busiest tramway line in Hungary (12-14 MGT/year, where MGT stands for million gross tons) but also one of the busiest in Europe. The site has R290 GHT rail quality installed; the welds and their surroundings bulged at several points on the bridge due to years and traffic loads, which were repaired by build-up welding on the running surface. Prior rail grinding was also performed on the entire section in question, resulting in a running surface hardness of 330-350 HB. The parameters of the straightness measuring beam are as follows:

- Type: SECNET DUAL;
- measurement base length: 1 m;
- simultaneous measurement of the running surface and the running edge;
- measuring range: $-2.5 \dots +1.5$ mm;
- accuracy: 0.05 mm in the measuring range.

The welds and their surroundings were measured (Fig. 4) and evaluated (Fig. 5) using a rail straightness measuring device, and the required weld lengths, typically 0.8-1.2 m, were determined. Figure 6 depicts one such failure location.

The embedding pouring was removed in the first step of the technology over the length to be welded + 0.1 m in both directions, on both sides of the rail, deep down to the bottom of the rail head (due to grinding and heat input, it is recommended to increase the removal length compared to the welding length - Fig. 7, Part A). Part 'B' depicts the surface prepared for welding; the preparation is done with the running surface cut out at 45° . Part 'C' depicts the condition following partial preheating (120°C). Part 'D' depicts the welded section with the weld layers applied. The following was the average number of layers deposited on the deposited length: 1-2 layers deposited at the weld's two edges, 2-3 layers deposited in and around the weld, and one layer removed on average during the finishing process (grinding). Table 5 shows the chemical composition of the filler metal used. Figure 8 depicts the finished welding after grinding.



Fig. 4 Rail straight measurement device

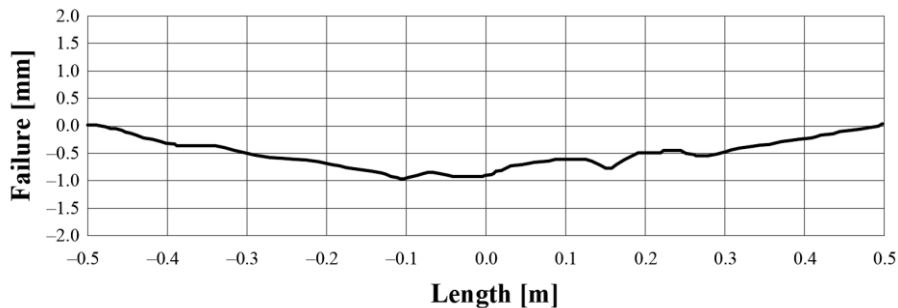


Fig. 5 Rail straight measurement protocol on the running surface



Fig. 6 Wear on the running surface at a welding in paved track

Table 5 Chemical composition of austenitic steel electrode for repairing the running surface

Chemical composition of weld metal [%]							
C	Si	Mn	Cr	Mo	Ni	Nb	Fe
0.1	0.5	6.0	19.0	0.2	8.5	< 0.1	64.5



Fig. 7 Technology steps. A – removed embedding pouring next to the rail head, B – preparing the surface, C – preheating, D – welding



Fig. 8 The completed welding after grinding

Visual inspection, geometric measurements, and surface hardness testing were used to monitor the sites after welding continuously. Visual inspection was performed to ensure that the weld had a solid, homogeneous structure, that no grinding defects had occurred during the finishing process, and that no cracks, material defects, or slag inclusions were visible.

For hardness measurement, a SAUTER HMO dynamic portable hardness tester (Fig. 9) was used, the main technical parameters of which are listed below [46]:

- complies with relevant DIN, EN, and ASTM standards, can be subject to accredited calibration;
- results can be displayed as HRC, HRB, HV, HB, HS and tensile strength values;
- accurate measurement results: ± 6 HLD;
- hardness scales: HL, HRB, HRC, HV, HB, HS;
- tensile strength U.T.S.: σ_b range from 375 to 2639 (steel only),
- accuracy: $\pm 1\%$ at 800 HL, ± 6 HLD;
- impact test: D (standard);
- optional sensors: DC, G;
- max. hardness value: 976 HV;
- min. specimen weight: 2-5 kg lifted, 0.05-2 kg attached;
- min. specimen thickness when attached: 8 mm;
- min. specimen bark thickness: 0.8 mm;
- dimensions: 135 mm \times 83 mm \times 24 mm.



Fig. 9 Hardness measurement device

The hardness tester reads hardness values (HLD) from the recoil rate using a Leeb scale, which can then be converted to the desired hardness value, e.g., HB, HV, and so on, and it can be used in most measuring positions (directions: ↓↙←↗↑).

The following observations were made following the hardness measurement tests: the pavement layers were crack-free, hardened quickly under traffic loads, and hardened more than the hardness of the connecting rail and wheels (320-350 HB) (Fig. 10). Transverse hardness measurements revealed that hardening was higher in areas more exposed to wheels and that transverse values were more dispersed than measurements made on rail base materials. The measurements also revealed that the number of layers influences the hardening degree. Hardness values were 15-20% lower in sections where 2-3 layers were welded (weld and its immediate surroundings) than in sections where 1-2 layers were welded (sections connected to the rail).

According to the measurements, the welded section reached 90-95% of the final hardness values in the first months. This equates to approximately 2-3 million through-rolled axle tons in this case.

The technology and filler material were also tested to repair previously repaired cracks during the experimental welds (Fig. 11). If the crack is in the rail head and does not spread to the rail web, it is possible to repair it. In this case, the authors discovered that it is suitable for crack repair at previously repaired locations (even for cracks that begin at these locations). Figure 11 depicts one such example.

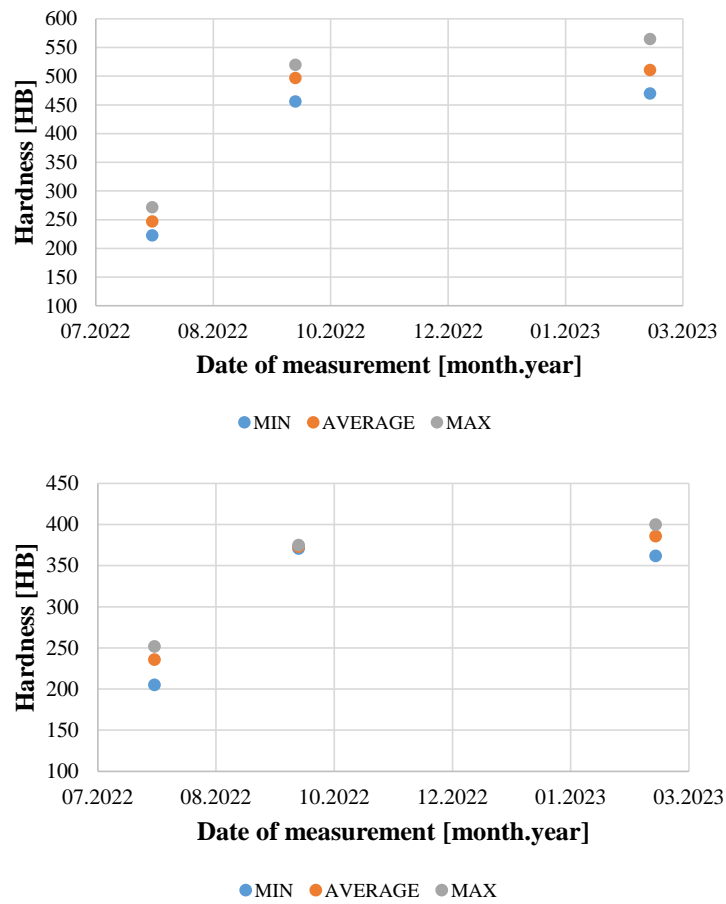


Fig. 10 Hardness values on the running surface at location #8 (top – rail, down – welding)



Fig. 11 Welding of a rail crack (left – crack, middle – preparing, right – completed welding)

The results were evaluated after the welds were completed and monitored; the main benefits and drawbacks are shown in Table 6.

Table 6 Advantages and disadvantages of the results

Advantages	Disadvantages
can be carried out during a night shift or even during traffic	more expensive consumables than hardfacing electrodes (but significantly cheaper overall)
lower demolition and restoration costs	excessive hardening (uneven wear, impact on the vehicle wheel)
less disruption to traffic than in the case of complete demolition	limited NDT inspection (magnetic principle instruments)
not susceptible to cracking	more significant deviation in hardness values in cross-sectional direction than hardfacing technology
reduced preheating time and costs	cannot be cut by flame

The first three advantages demonstrate that the chosen method is unquestionably advantageous from a railway operator and economic standpoint.

However, because the hardness values were significantly higher than those of the rails and vehicle wheels, additional research was conducted to determine the number of layers that would result in a hardness close to that of the rails and vehicle wheels while remaining technically and economically feasible. According to the findings, hardening occurs according to a power or logarithmic function.

The hardness values for single-layer welds are clearly higher due to the carbon added from the base material, whereas the hardness values for two-layer welds are lower. As a result, the goal was to create a technology that met the following criteria:

1. technology that can be used with partial preheating (~80-120 °C);
2. without or with minimum demolition of the paved track;
3. use of crack insensitive filler (Table 5);
4. hardness is still equal to or greater than rails and welds.

Following that, a testing site was chosen that met the following criteria: sufficient rail wear (on the running surface) to determine different layer numbers and excavation depths and a site with paved track to test an even more limited preheating technology. In this case, only the deepest section (about 70% of the total length) was preheated to allow the less worn section to heat up due to the heat input during welding. Furthermore, a section adjacent to this site was chosen where a reference section was repaired using conventional hardfacing technology in addition to stripping.

Other important considerations included the sections' high traffic volume and the fact that the sites had previously been repaired using hardfacing technology, which is no longer feasible, and track replacement is not feasible. This will demonstrate that the chosen solution can extend the track's technical lifetime.

The location was once again on the same line as the previous measurements (Fig. 12). The austenitic drift technology received a 1.2 m long section, while the hard-applied technology received a 0.8 m long section.

Figure 13 illustrates the limited preheating in this section.

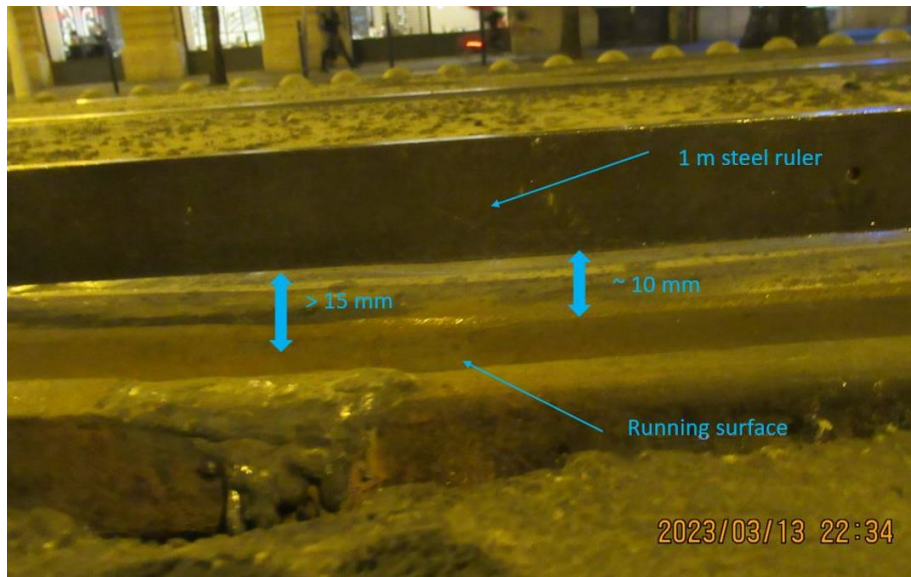


Fig. 12 The selected location for austenitic build-up welding



Fig. 13 Partial preheating on the selected location

Because of the weld defects, the authors were able to inspect 1-6 weld layers together on site. The welds were completed on March 14, 2023, with the following technological parameters:

- base material: 2.2 according to ISO TR 15608 [47];
- steel grade: R260 GHT according to EN 14811 [29];

- welding process: 111 – Manual metal arc welding according to ISO 4063 [48];
- welding position: PA according to ISO 6947:2019 [49];
- build-up welding;
- filler metal: E Fe 10 according to EN 14700 [50] or 1.4370 Material No.;
- electric current type: DC (+) / AC;
- diameter: 6 mm, length 450 mm;
- amperage: 220-250 A;
- preheating: 120 °C;
- examination: VT (visual testing), geometry measurement.

4. RESULTS

The hardness values of the completed welds were measured every 5 cm on the running surface. To obtain more accurate results, several measurements were taken weekly at first; then, when the hardening rate began to slow, the measurements were changed to weekly and bi-weekly, and when the hardness values became relatively stagnant, a control measurement was taken after six weeks. This happened again after more than two months. The authors intend to examine this section further in the future. In addition to hardness measurements, the following tests were performed: visual inspection of the weld, straightness measurement with a steel ruler, hardness measurement on the tread transversely every 0.05 m, and a penetration test if necessary. It should be noted that, despite the weld being hardened during forming, there was no change in the initial geometry during hardening.

Table 7 shows the measurement days and the corresponding through-rolled axle load data in tonnes.

Table 7 Measurement dates and axle loads in tons

Date [day.month.year]	Through-rolled axle tons [tons]
14.03.2023	9,450
16.03.2023	70,560
20.03.2023	196,740
24.03.2023	349,020
31.03.2023	589,680
06.04.2023	807,300
21.04.2023	1,311,660
05.05.2023	1,792,980
19.05.2023	2,274,300
29.06.2023	3,679,920
25.08.2023	5,643,270

Based on Fig. 2, the average hardness values of the austenitic and control hardfacing welds are shown in Figs. 14 and 15, respectively. A consumable with the chemical composition shown in Table 8 was used for the control hardfacing, and the preheating temperature was set to 350 °C. The base materials in both cases were R260 GHT grooved rails.

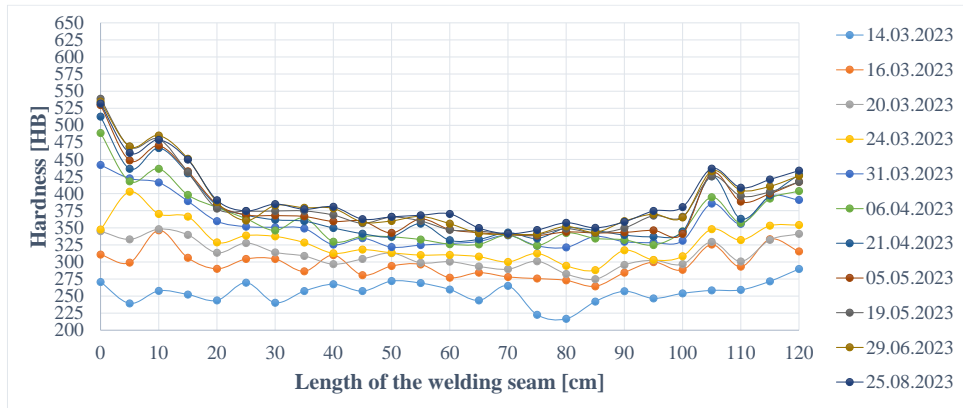


Fig. 14 Austenitic build-up welding hardness (average values)

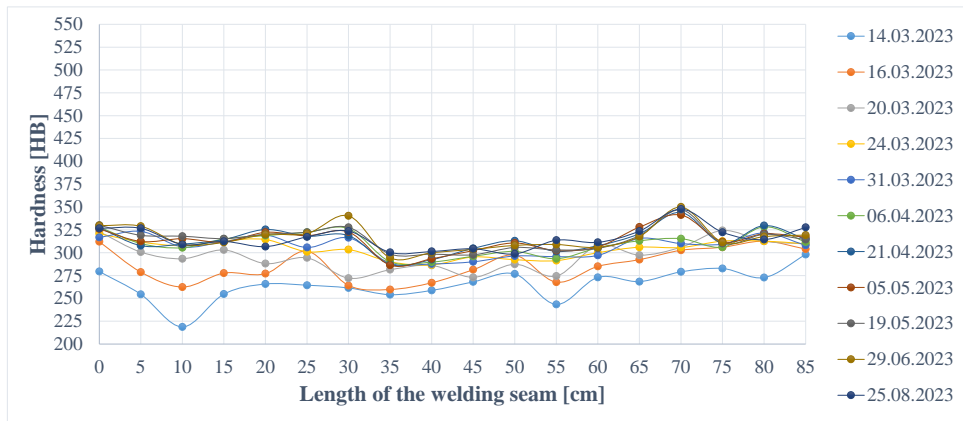


Fig. 15 Hardfacing build-up welding hardness (average values)

Table 8 Hardfacing stick electrode chemical composition

Chemical composition in % of weld metal				
C	Si	Mn	Cr	Fe
0.15	1.10	1.20	0.80	Balanced

5. DISCUSSION

The findings clearly show that, in the case of a hardfacing technology, deformation-induced hardening in the railway track is negligible, regardless of the number of layers used. Hardening of about 15-18% (45 HB) was observed in the first month under an axle load of 600,000-800,000 tonnes, which remained essentially unchanged thereafter, and under further loads - significant for the period under study - the hardness of the applied layer hardly increased at all, with a maximum increase of 7-10 HB (1-2% increase). Previous operator experience confirms that after 20-30 years in service, R260 grade rails harden to this value.

The authors obtain much more interesting results for austenitic build-up welding. Before delving into the data, it is worth noting that while there were no outliers between the average and maximum values for conventional hard surfacing, the variance was more remarkable for the austenitic layer, with maximum values on the running surface being 4-8% (15-20 HB) higher than the average values. The running surface here showed a greater divergence between the parts of the running surface that were constantly in contact with the vehicle wheel and the surfaces that were not in contact with the wheel, whereas this phenomenon was scarce on the hardfacing layers. The diagram also clearly shows that high hardness values could be measured on the two edges of the seam as a result of the carbon picked up from the base material and faster cooling, particularly on the left side of the seam, where the depth of wear and preparing was less than on the right side. Hardness values of 520-550 HB are not uncommon in the former case, while hardness values in the latter case increased above 400 HB. The section between 30-95 cm roughly corresponded to the previously expected and predicted 340-380 HB values. This range is very close to the hardened normal R260 rail quality and the hardness of the heat-treated rails, and it is also very close to the hardness of the vehicle wheels, resulting in optimal wheel-rail interaction. It is also worth noting that the number of layers used in this width range varied between 2 and 6, but the hardness values did not decrease significantly as the number of layers increased. As a result, with two or more layers of welds, the number of welds has no significant effect on hardening, and there are no significant differences in hardness values. This condition develops after approximately 3.5 million tonnes of axle load. The graph also shows that the initial period (the first 0.5 million tonnes) shows a more significant hardening, followed by a steadily slowing rate. The stirring of the carbon and the rapid cooling caused by partial preheating cause critical hardening of the joint sections, which may remain more prone to cracking in the case of 1-layer welds. Laboratory tests to determine the amount of martensite formed could be part of future research. The deposited layer in the multi-layer sections remained austenitic (non-magnetizable).

Table 9 summarizes the approximate hardening curves determined for each measurement cross-section as a function of traffic load.

Table 9 Regression functions for the hardness on each cross-section by austenitic welding (H_e is the estimated Brinell hardness on the running surface [HB], t is the through-rolled axle tons [tons]).

Nr. of the cross-section	Equation of the regression function	R ²
#1	$H_e = 77.577 \times t^{0.1289}$	0.904
#2	$H_e = 88.392 \times t^{0.1122}$	0.941
#3	$H_e = 103.14 \times t^{0.1035}$	0.952
#4	$H_e = 105.42 \times t^{0.0967}$	0.981
#5	$H_e = 121.26 \times t^{0.0789}$	0.943
#6	$H_e = 170.31 \times t^{0.0530}$	0.930
#7	$H_e = 131.26 \times t^{0.0716}$	0.959
#8	$H_e = 139.79 \times t^{0.0667}$	0.958
#9	$H_e = 156.11 \times t^{0.0570}$	0.925
#10	$H_e = 149.66 \times t^{0.0588}$	0.971
#11	$H_e = 171.58 \times t^{0.0488}$	0.963
#12	$H_e = 158.91 \times t^{0.0550}$	0.945
#13	$H_e = 150.58 \times t^{0.0571}$	0.981
#14	$H_e = 147.52 \times t^{0.0575}$	0.960
#15	$H_e = 167.66 \times t^{0.0483}$	0.854
#16	$H_e = 128.14 \times t^{0.0671}$	0.931
#17	$H_e = 107.88 \times t^{0.0804}$	0.945
#18	$H_e = 129.14 \times t^{0.0666}$	0.891
#19	$H_e = 153.14 \times t^{0.0560}$	0.982
#20	$H_e = 139.48 \times t^{0.0638}$	0.955
#21	$H_e = 140.50 \times t^{0.0636}$	0.970
#22	$H_e = 118.76 \times t^{0.0870}$	0.957
#23	$H_e = 123.56 \times t^{0.0779}$	0.969
#24	$H_e = 150.62 \times t^{0.0679}$	0.937
#25	$H_e = 147.15 \times t^{0.0715}$	0.942

The measured hardness functions for all 25 cross-sections are presented in Fig. 16, as are the calculated average function and the corresponding power regression function (see Table 9).

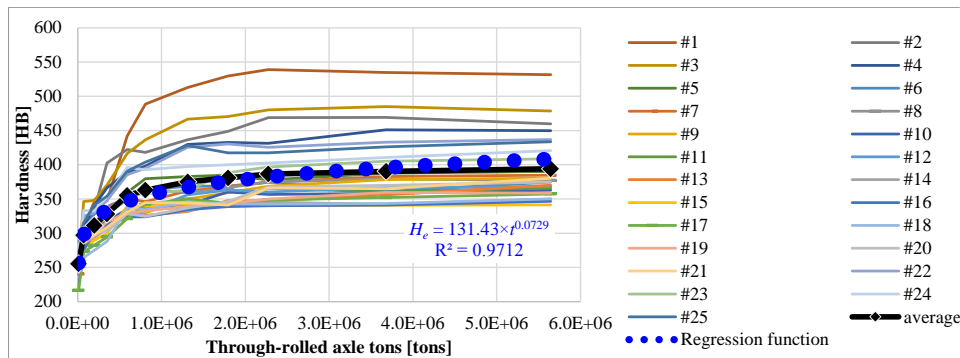


Fig. 16 Measured hardness values of all cross-sections (from #1 to #25) on the running surface in the case of austenitic welding, as well as the calculated average function and the corresponding power regression function

Best-fit equations were also examined for 3.5 and 5.5 million tons. The power function, rather than the logarithmic approach, provided the best correlation in both cases.

The power functions had an average $R^2=0.951$ after 3.5 million tons of axle load, while the logarithmic equations had $R^2=0.944$, a ratio that became even closer after more than 5.5 million tons of loading: power $R^2=0.946$, and logarithmic function $R^2=0.944$. The authors intend to pursue their research in the long term, and the power function may no longer be the best-fitting function in the future.

The following formula (Eq. (1)) gives the best approximation for multi-layer (at least 2-3 layers) welding up to nearly 6 million tons of load when the hardness values of each cross-section are considered as a function of the axial load.

$$H_e = 150 \times t^{0.0575} \quad (1)$$

It should be noted that the equation for one-layer welding is not shown because this solution should be avoided. It should also be mentioned that the equation in Fig. 16 is related to the average of all cross-sections, which includes everything from single-layer welds to multi-layer welds. Because the remaining seam layers #2...#4 are technically and economically the best solution, only the seams in this range are considered in the equation, which is most typical for seams #9...#17, and a conclusion is drawn from the equations with the best R^2 values (see Eq. (1)).

6. CONCLUSIONS

Based on the findings, it is possible to conclude that a crack-insensitive welding technology can be used for the permanent repair of most rail qualities.

Based on the above results, a minimum of 2-3 layers (remaining after grinding) can be determined, for which additional parameters can be defined. The preheating temperature has already been mentioned; the grinding angle should be 45° to the rail's running surface (where the machined part meets the intact material's running surface). Grinding can be done with a tool, such as a milling (grinding) machine. The ideal preparation depth is 5-10 mm, and it must be uniform across the entire length to be welded. A more significant flaw can be used, but preparation along the entire length is difficult and potentially time-consuming. When welding paved tracks, the embedding pouring must be removed from both sides of the rail head, at least up to the bottom, over a length of -10 to $+10$ cm. The electrode diameters used are 4, 5, and 6 mm, with a seam height ranging from 2-3 mm to 4-6 mm. Due to slower welding, smaller electrode diameters allow more heat to remain in the system, preventing rapid cooling. It should be noted that the first layer deposited is typically slightly thinner than the thicknesses described above. Two rows of welds should always be welded at 45° joints to avoid cracking at the edges of the welds. To avoid end craters, weld the trapezoidal mold's edges according to the numbered orange seams shown in Fig. 17 (seams 1 to 4, including double seams 1 and 3), and a 1 to 1 seam is sufficient in the longitudinal direction. After welding the prepared part's edges, the rows of red seams can be laid down in layers (5 to n) using one-way welding (for heat conduction) to avoid slag trapping.

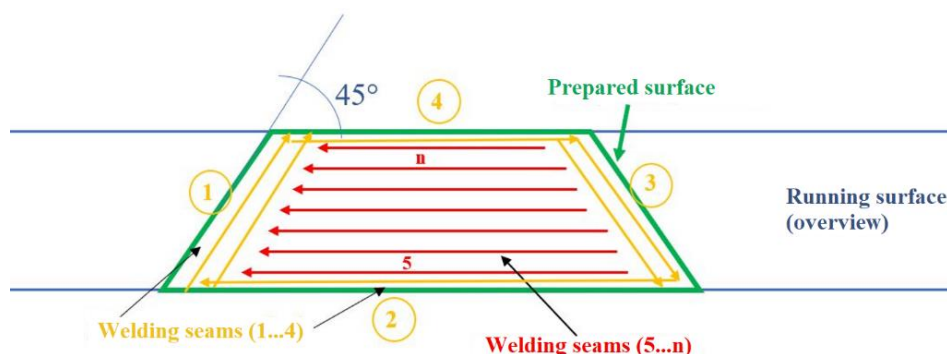


Fig. 17 Welding seams on the running surface

Finally, the results obtained can provide numerous benefits to the railway infrastructure industry, both operationally and economically. Nonetheless, there is still much room for more research in the field under consideration, both on the ground and in the lab. Further investigation of hardening in traffic at the designated locations may be required, which should result in a more precise determination of the hardening correlation and provide helpful information for calculating life expectancy.

Acknowledgement: This paper was technically supported by the research team entitled "SZE-RAIL".

REFERENCES

1. Kurhan, M.B., Kurhan, D.M., Husak, M.A., Hmelevska, N., 2022, *Innovative Technologies for the Introduction of High-Speed Train Operation (on the Example of Track Maintenance in the Plan)*, Transport Means - Proceedings of the International Conference, Kaunas, 2022, 185103.
2. Gaál, B., Horváth, B., 2017, *System Approach for Strategic Planning in Transport*, Acta Technica Jaurinensis, 10(1), pp. 13-20.
3. Bokor, Z., Horváth, B., 2015, *Upgrading Multilevel Full Cost Allocation: Case Transport*, Acta Technica Jaurinensis, 8(4), pp. 312-319.
4. Blagojević, A., Stević, Ž., Marinković, D., Kasalica, S., Rajilić, S., 2020, *A novel entropy-fuzzy PIPRECIA-DEA model for safety evaluation of railway traffic*, Symmetry, 12(9), 1479.
5. Dobruszkes, F., 2011, *High-speed rail and air transport competition in Western Europe: A supply-oriented perspective*, Transport Policy, 18(6), pp. 870-879.
6. Macura, D., Laketić, M., Pamučar, D., Marinković, D., 2022, *Risk Analysis Model with Interval Type-2 Fuzzy FMEA—Case Study of Railway Infrastructure Projects in the Republic of Serbia*, Acta Polytechnica Hungarica, 19(3), pp. 103-118.
7. Ramazan, B., Mussaliyeva, R., Bitileuova, Z., Naumov, V., Taran, I., 2021, *Choosing the logistics chain structure for deliveries of bulk loads: Case study of the Republic Kazakhstan*, Naukovyi Visnyk Natsionalnoho Hirnychoho Universytetu, 2021(3), pp. 142-147.
8. Nugymanova, G., Nurgaliyeva, M., Zhanbirov, Z., Naumov, V., Taran, I., 2021, *Choosing a servicing company's strategy while interacting with freight owners at the road transport market*, Naukovyi Visnyk Natsionalnoho Hirnychoho Universytetu, 2021(1), pp. 204-210.
9. Kocsis Szürke, S., Sütthő, G., Apagyi, A., Lakatos, I., Fischer, S., 2022, *Cell Fault Identification and Localization Procedure for Lithium-Ion Battery System of Electric Vehicles Based on Real Measurement Data*, Algorithms, 15(12), 467.

10. Kocsis Szürke, S., Kovács, G., Sysyn, M., Liu, J., Fischer, S., 2023, *Numerical Optimization of Battery Heat Management of Electric Vehicles*, Journal of Applied and Computational Mechanics, 9(4), pp. 1076-1092.
11. Mohammed, D., Horváth, B., 2023, *Travel Demand Increment Due to the Use of Autonomous Vehicles*, Sustainability, 15(11), 8937.
12. Lajunen, A., Lipman, T., 2016, *Lifecycle cost assessment and carbon dioxide emissions of diesel, natural gas, hybrid electric, fuel cell hybrid and electric transit buses*, Energy, 106, pp. 329-342.
13. Kocsis Szürke, S., Dineva, A., Szalai, S., Lakatos, I., 2022, *Determination of critical deformation regions of a lithium polymer battery by dic measurement and wowa filter*, Acta Polytechnica Hungarica, 19(2), pp. 113-134.
14. Dineva, A., Csomós, B., Kocsis Szürke, S., Vajda, I., 2021, *Investigation of the performance of direct forecasting strategy using machine learning in State-of-Charge prediction of Li-ion batteries exposed to dynamic loads*, Journal of Energy Storage, 36, 102351.
15. Horváth, B., Szép, J., Borsos, A., 2023, *The Concept of BENIP-Built Environment Information Platform*, Infocommunications Journal, 2023, pp. 29-34.
16. Okechukwu, C., Dahunsi, O.A., Oke, P.K., Oladele, I.O., Dauda, M., 2017, *Prominence of Hadfield Steel in Mining and Minerals Industries: A Review*, International Journal of Engineering Technologies, 3(2), pp. 83-90.
17. Gürol, U., Karahan, T., Erdöl, S., Çoban, O., Baykal, H., Koçak, M., 2022, *Characterization of Armour Steel Welds Using Austenitic and Ferritic Filler Metals*, Transactions of the Indian Institute of Metals, 75(3), pp. 757-770.
18. Molyneux-Berry, P., Davis, C., Bevan, A., 2014, *The influence of wheel/rail contact conditions on the microstructure and hardness of railway wheels*, The Scientific World Journal., 2014, 209752.
19. Liu, P., Quan, Y., Wan, J., Yu, L., 2021, *Experimental investigation on the wear and damage behaviors of machined wheel/rail materials under dry sliding conditions*, Materials, 14(3), 540.
20. Bozkurt, F., 2023, *Investigation of Tribological Properties of Head, Web and Foot Sections of R260 Rail*, Demiryolu Mühendisliği, 2023(17), pp. 107-114.
21. Protsenko, P., Borodii, Y., Bobyr, M., Uhlmann, E., Thalau, J., Lypovka, P., 2019, *The wear resistance research of the rail contact surface depending on the grinding process*, Mechanics and Advanced Technologies, 2(86), pp. 14-22.
22. Viana, T.G., Tressia, G., Sinatora, A., 2020, *Sliding wear of rail and wheel steels: Effect of hardness ratio, normal load and lubrication*, Tribology in Industry, 42(3), pp. 428-442.
23. Lakušić, S., Ahac, M., 2012, *Hardness distribution over cross-section of grooved rails*, Građevinar, 64(12), pp. 1009-1018.
24. Poznyakov, V.D., Kiriakov, V.M., Gajvoronsky, A.A., Klapatyuk, A.V., Shishkevich, O.S., 2010, *Properties of Welded Joints of Rail Steel in Electric Arc Welding*, The Paton Welding Journal, 8, pp. 16-20.
25. Konstantinova, M.V., Balanovskiy, A.E., Gozbenko, V.E., Kargapoltsev, S.K., Karlina, A.I., Shtayger, M.G., Guseva, E.A., Kuznetsov, B.O., 2019, *Application of plasma surface quenching to reduce rail side wear*, IOP Conference Series: Materials Science and Engineering, 560(1), 012146.
26. Woodhead, D.H., 2021, *Investigating the performance of rail steels*, Fields Journal of Huddersfield student research, 7(1), pp. 1-15.
27. Kurhan, M., Kurhan, D., Novik, R., Baydak, S., Hmelevska, N., 2020, *Improvement of the railway track efficiency by minimizing the rail wear in curves*, IOP Conference Series: Materials Science and Engineering, 985(1), 012001.
28. European Committee for Standardization, 2011, *EN 13674-1:2011, Railway applications. Track. Rail. Part 1: Vignole railway rails 46 kg/m and above*, 123 p.
29. European Committee for Standardization, 2019, *EN 14811:2019, Railway applications - Track - Special purpose rail - Grooved rails and associated construction profiles*, 104 p.
30. Kou, L., 2022, *A Review of Research on Detection and Evaluation of the Rail Surface Defects*, Acta Polytechnica Hungarica, 19(3), pp. 167-186.
31. Krishna, V.V., Hossein-Nia, S., Casanueva, C., Stichel, S., 2020, *Long term rail surface damage considering maintenance interventions*, Wear, 460-461, 203462.
32. Bajic, D., Vladimirovich Kuzmenko, G., Samardzic, I., 2013, *Welding of rails with new technology of arc welding*, Metalurgija., 52(3), pp. 399-402.
33. Aksenova, K., Gromov, V., Ivanov, Y., Qin, R., Vashchuk, E., 2022, *Structural Phase Transformation of Rail Steel in Compression*, Metals, 12(11), 1985.

34. Protsenko, P., Borodii, Y., Petryshyn, A., Thalau, J., Lypovka, P., Uhlmann, E., Horbyk, V., Hlukhovskiy, V., 2019, *The Research of the Railway Rail for Analysis of Surface Initiated Rolling Contact Fatigue Cracks*, Mechanics and Advanced Technologies, 1 (88), pp. 19-28.
35. Seo, J.W., Hur, H.M., Kwon, S.J., 2022, *Effect of Mechanical Properties of Rail and Wheel on Wear and Rolling Contact Fatigue*, Metals, 12(4), 630.
36. Zaitseva, T.I., Blinova, I.V., Uzdin, A.M., 2020, *Dynamics of welded rails gap and hardness of rail base*, International Journal of Applied Mechanics and Engineering., 25(1), pp. 236-242.
37. Gertsyk, S., Volgina, N., 2020, *Causes of destruction of continuous welded rail tracks*, 2020, MATEC Web of Conferences, ICMTMTE 2020, Sevastopol, 329, 03046.
38. Fischer, S., Harangozó, D., Németh, D., Kocsis, B., Sysyn, M., Kurhan, D., Brautigam, A., 2023, *Investigation of heat-affected zones of thermite rail weldings*, Facta Universitatis Series Mechanical Engineering, doi: <https://doi.org/10.22190/FUME221217008F>.
39. Jovanović, V., Janošević, D., Marinković, D., Petrović, N., Pavlović, J., 2023, *Railway Load Analysis During the Operation of an Excavator Resting on the Railway Track*, Acta Polytechnica Hungarica, 20(1), pp. 79-93.
40. Tica, M., Vrcan, Ž., Troha, S., Marinković, D., 2023, *Reversible planetary gearsets controlled by two brakes, for internal combustion railway vehicle transmission applications*, Acta Polytechnica Hungarica, 20(1), pp. 95-108.
41. Monek, G., Fischer, S., 2023, *DES and IIoT fusion approach towards real-time synchronization of physical and digital components in manufacturing processes*, Reports in Mechanical Engineering, 4(1), pp. 161-174.
42. Ovchinnikov, D., Bondarenko, A., Kou, L., Sysyn, M., 2021, *Extending service life of rails in the case of a rail head defect*, Gradevinar, 73(2), pp. 119-125.
43. Pultznerová, A., Mečár, M., Šestáková, J., Hodás, S., 2022, *Influence of the Condition of the Railway Superstructure on Traffic Noise on the Regional Line*, Civil and Environmental Engineering Reports, 18(2), pp. 402-407.
44. Kampczyk, A., Gamon, W., Gawlak, K., 2023, *Integration of Traction Electricity Consumption Determinants with Route Geometry and Vehicle Characteristics*, Energies, 16(6), 2689.
45. Fischer, S., 2015, *Traction Energy Consumption of Electric Locomotives and Electric Multiple Units at Speed Restrictions*, Acta Technica Jaurinensis, 8(3), pp. 240-256.
46. <https://grimas.hu/termek/sauter-hmo-dinamikus-hordozhato-kemenysegmero> (last access: 30.08.2023)
47. International Organization for Standardization, 2017, *ISO/TR 15608:2017, Welding – Guidelines for a metallic materials grouping system*, 7 p.
48. International Organization for Standardization, 2023, *ISO 4063:2023, Welding, brazing, soldering and cutting – Nomenclature of processes and reference numbers*, 7 p.
49. International Organization for Standardization, 2019, *ISO 6947:2019, Welding and allied processes. Welding positions*, 28 p.
50. European Committee for Standardization, 2014, *EN 14700:2014, Welding and allied processes*, 14 p.